Comparative Analysis of Homology Models of the Ah Receptor Ligand Binding Domain: Verification of Structure–Function Predictions by Site-Directed Mutagenesis of a Nonfunctional Receptor

Domenico Fraccalvieri,[†] Anatoly A. Soshilov,[‡] Sibel I. Karchner,[§] Diana G. Franks,[§] Alessandro Pandini,[∥] Laura Bonati,[†] Mark E. Hahn,[§] and Michael S. Denison*[,‡]

[†]Department of Earth and Environmental Sciences, University of Milano-Bicocca, Milan, Italy
[‡]Department of Environmental Toxicology, Meyer Hall, University of California, Davis, California 95616, United States
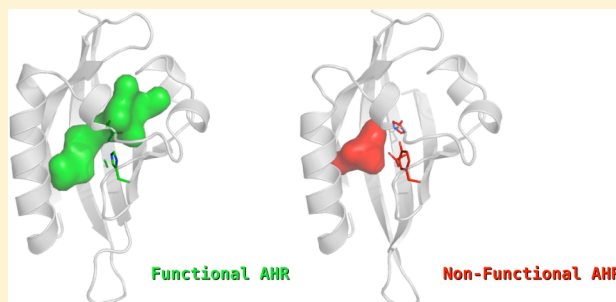[§]Biology Department, Woods Hole Oceanographic Institution, Woods Hole, Massachusetts 02543, United States
[∥]Randall Division of Cell and Molecular Biophysics, King's College London, London, U.K.

Ⓢ Supporting Information

ABSTRACT: The aryl hydrocarbon receptor (AHR) is a ligand-dependent transcription factor that mediates the biological and toxic effects of a wide variety of structurally diverse chemicals, including the toxic environmental contaminant 2,3,7,8-tetrachlorodibenzo-p-dioxin (TCDD). While significant interspecies differences in AHR ligand binding specificity, selectivity, and response have been observed, the structural determinants responsible for those differences have not been determined, and homology models of the AHR ligand-binding domain (LBD) are available for only a few species. Here we describe the development and comparative analysis of homology models of the LBD of 16

Functional AHR   **Non-Functional AHR**

AHRs from 12 mammalian and nonmammalian species and identify the specific residues contained within their ligand binding cavities. The ligand-binding cavity of the fish AHR exhibits differences from those of mammalian and avian AHRs, suggesting a slightly different TCDD binding mode. Comparison of the internal cavity in the LBD model of zebrafish (zf) AHR2, which binds TCDD with high affinity, to that of zfAHR1a, which does not bind TCDD, revealed that the latter has a dramatically shortened binding cavity due to the side chains of three residues (Tyr296, Thr386, and His388) that reduce the amount of internal space available to TCDD. Mutagenesis of two of these residues in zfAHR1a to those present in zfAHR2 (Y296H and T386A) restored the ability of zfAHR1a to bind TCDD and to exhibit TCDD-dependent binding to DNA. These results demonstrate the importance of these two amino acids and highlight the predictive potential of comparative analysis of homology models from diverse species. The availability of these AHR LBD homology models will facilitate in-depth comparative studies of AHR ligand binding and ligand-dependent AHR activation and provide a novel avenue for examining species-specific differences in AHR responsiveness.

The aryl hydrocarbon receptor (AHR) is a ligand-dependent basic helix–loop–helix (bHLH)/Per-ARNT-Sim (PAS) domain-containing transcription factor that regulates gene expression and other cellular signaling events.[1–3] Mechanistically, binding of ligand to the AHR in the cytosol of a cell stimulates translocation of the AHR protein complex to the nucleus and its subsequent dimerization with the ARNT (AHR nuclear translocator) protein transforms the ligand–AHR–ARNT complex into its high-affinity DNA binding form.[3–5] Binding of the ligand-activated AHR complex to its specific DNA recognition site, the dioxin responsive element (DRE), stimulates transcription of adjacent genes and thus mediates the toxic and biological effects of AHR ligands.[1,3]

Unlike many nuclear receptors, the AHR can bind and be activated by a wide variety of structurally diverse natural and synthetic compounds,[6–9] including halogenated aromatic hydrocarbons (HAHs) such 2,3,7,8-tetrachlorodibenzo-p-dioxin (TCDD, dioxin), and the spectrum of biological and toxic effects produced by the ligand-activated AHRs is dependent upon the physicochemical characteristics and metabolic persistence of the ligand.[3,7,10] More recent studies have reported that the ligand binding promiscuity of a given AHR may result from differential binding of structurally diverse ligands within the AHR ligand-binding cavity,[11–14] similar to the mechanisms responsible for pregnane X receptor ligand binding promiscuity.[15,16]

Table 1. AHR Sequences Selected for Comparative Analysis

	species	form	label	NCBI accession no.	TCDD affinity	ref(s)
mammals	mouse C57BL/6 (*Mus musculus*)	AHR1	mAHR	NP_038492	high	52, 55
	rat (*Rattus norvegicus*)	AHR1	rtAHR	AAA56897	high	55
	hamster (*Mesocricetus auratus*)	AHR1	haAHR	AAF87578	high	55
	rabbit (*Oryctolagus cuniculus*)	AHR1	rbAHR	O02747	high	55
	guinea pig (*Cavia porcellus*)	AHR1	gpAHR	AAT35817	high	55
	beluga whale (*Delphinapterus leucas*)	AHR1	bAHR	AAL04031	high	54
	harbor seal (*Phoca vitulina*)	AHR1	sAHR	BAB64569	high	56
	mouse DBA/2J (*Mus* sp.)	AHR1	mDBA AHR	AAB32339	medium	57
	human (*Homo sapiens*)	AHR1	huAHR	NP_001612	medium	52
birds	chicken (*Gallus gallus*)	AHR1	chAHR	NP_989449	high	53
	common tern (*Sterna hirundo*)	AHR1	tAHR	AAF15281	medium/low	53
fish	zebrafish (*Danio rerio*)	AHR2	zfAHR2	NP_571339	high	29
	zebrafish (*D. rerio*)	AHR1b	zfAHR1b	NP_001019987	medium	29
	killifish (*Fundulus heteroclitus*)	AHR1a	kfAHR1a	AAR19366	low	60
	killifish (*F. heteroclitus*)	AHR2a	kfAHR2a	AAC59696	medium	unpublished work of M. E. Hahn
	zebrafish (*D. rerio*)	AHR1a	zfAHR1a	NP_571103	no binding	28, 29, unpublished work of M. E. Hahn

While the lack of any three-dimensional structure information about the AHR ligand binding domain (LBD) has prevented detailed molecular analysis of the mechanisms of AHR ligand binding, we and others have used the availability of crystal and nuclear magnetic resonance (NMR) structures of homologous protein domains to develop homology models of the AHR LBD for such analysis.[12,17−20] These theoretical models not only have revealed key structural aspects of the domain but also, when coupled with site-directed mutagenesis and functional analysis, have proven to be helpful in identifying amino acids that are important in ligand binding and ligand-dependent AHR activation.[12,17−19,21] More recently, these models have been used in molecular docking studies in an attempt to elucidate the detailed interactions of some known ligands (agonists) within the AHR LBD as well as in the virtual screening of collections of putative ligands.[12,18−20,22−25] While the binding modes of TCDD and other ligands within the AHR LBD of a given species (typically that of mouse or human AHR) have been predicted by these approaches, experimental confirmation of these proposed interactions is generally lacking. Moreover, until recently, modeling studies have been focused on a limited number of species.[12,17−20] The availability of homology models for the AHR LBD from a wide variety of species would provide avenues not only for further investigation of basic mechanisms of ligand binding and AHR activation but also for examination of mechanisms and structural determinants responsible for the dramatic intra- and interspecies differences that have been observed in AHR ligand binding, ligand selectivity, and response.[3,10,14,26,27]

Accordingly, here we describe the development and comparative analysis of homology models of the LBD of 16 AHRs from 12 mammalian and nonmammalian species. By comparing the volume and shape of the binding cavities in different AHRs, as well as the physicochemical properties of the internal residues, we inferred the role of amino acids that are known to affect TCDD binding affinity. To further assess the value of this approach in predicting structure−function relationships, we focused on experimental verification of residues predicted to be important in determining the functional attributes of a fish AHR. Zebrafish (*Danio rerio*) possess three AHRs, one of which (AHR1a) has been shown previously to lack the ability to bind TCDD and DNA and to activate transcription in the presence of TCDD.[28,29] Structural modeling of representative fish AHRs was used to guide site-directed mutagenesis and functional analysis in identifying the specific residues within the zebrafish AHR1a LBD that contribute to its inability to bind TCDD or exhibit TCDD-dependent DNA binding activity. On this basis, zfAHR1a mutants designed to restore TCDD responsiveness were prepared and experimentally validated, demonstrating the key role of these residues and highlighting the predictive value of the comparative modeling analysis. The proposed approach not only will further contribute to elucidating the mechanisms of AHR ligand binding but also will provide additional insights into the diversity of AHR ligands and the species-specific differences in AHR responsiveness.

■ EXPERIMENTAL PROCEDURES

Homology Modeling. The PASB ligand binding domain (LBD) structures of 16 mammalian, avian, and fish AHRs (Table 1) were generated by homology modeling following our previously described protocol.[17,18] Briefly, template identification by sequence similarity was performed independently for each target sequence using PSI-BLAST[30] against the Protein Data Bank (PDB)[31] with default parameters. For all targets, the top hits were the PASB domains of hypoxia-inducible factor 2α (HIF-2α) and ARNT. NMR structures of HIF-2α (PDB entry 1P97[32]) and ARNT (PDB entry 1X0O[33]) were chosen, and the most representative structure in the NMR ensemble of each template was selected using NMRCLUST.[34] The two templates were structurally aligned with DALI-Lite.[35,36] For each AHR, the target−template sequence alignment was generated with CLUSTALW,[37,38] and the result was confirmed using the Align-2D command within MODELLER.[39−41] Models of each AHR LBD were built with MODELLER version 8v1,[39−41] a program that implements comparative modeling by satisfying spatial restraints. One hundred candidate models were derived for each target, and the optimal model that was selected was that with the lowest value of the objective function. The quality of the obtained models was assessed with PROCHECK,[42] which provides information about the stereochemical quality, and by the ProSA validation method,[43,44] which evaluates model accuracy and statistical significance with a knowledge-based potential. Secondary structures were attributed by

DSSPcont.[45] This program extends the discrete assignments of secondary structure performed by DSSP[46] to a continuous assignment in the same categories providing increased accuracy. The continuum results are calculated by weighted averages over 10 discrete DSSP assignments with different hydrogen bond thresholds. Three-dimensional visualization and images of the resulting AHR LBD structures were generated using PyMOL.[47]

Analysis of Structural Cavities. Identification and characterization of surface pockets and internal cavities in each of the modeled structures were performed with the CASTp server.[48] This program allows identification and calculation of the Connolly's molecular surface and volume for all pockets and cavities in a protein structure. It ranks the cavities by size, where the largest one is usually the binding site. The representations of the resulting cavity surfaces were produced with PyMOL.[47]

Chemicals. [³H]TCDD (>99% radiochemical purity) was obtained from Chemsyn Science Laboratories (Lenexa, KS) or was a kind gift from S. Safe (Texas A&M University, College Station, TX). [³⁵S]Methionine was purchased from Amersham (Piscataway, NJ) or Perkin-Elmer (Waltham, MA), and [γ-³²P]ATP was from Perkin-Elmer.

Plasmids. The zebrafish AHR1b (zfAHR1b) expression construct pcDNA-zfAHR1b was described previously.[29] Expression constructs for zebrafish AHR1a, AHR2, ARNT2b, and ARNT1c (pBKCMV-zfAHR1a, pBKCMV-zfAHR2, pBKCMV-zfARNT2b, and pBKCMV-zfARNT1c, respectively)[28,49,50] were generously provided by R. Tanguay (Oregon State University, Corvallis, OR) and R. E. Peterson (University of Wisconsin, Madison, WI). In the course of sequencing the pBKCMV-zfAHR1a plasmid, seven single-nucleotide differences in the zfAHR1a cDNA sequence from that of the GenBank zfAHR1a sequence were identified, including two nonsynonymous differences resulting in L129I and P280T substitutions in the zfAHR1a protein.

zfAHR1a Site-Directed Mutagenesis, in Vitro Protein Synthesis, and Functional Analysis. Three amino acid residues (296, 386, and 388) in the ligand-binding domain of zfAHR1a were mutated using the QuikChange XL site-directed mutagenesis kit (Stratagene), following the manufacturer's instructions. The pBKCMV-zfAHR1a plasmid was amplified with Pfu polymerase; the complementary primer pairs used for each mutated site are included in the Supporting Information (Table S1). The zf1-3868/zf1-c3868 primer pair was used to generate a double mutant zfAHR1a at residues 386 and 388. A splicing approach was used to generate the double mutations at positions 296 and 386 and positions 296 and 388 and the triple mutation at positions 296, 386, and 388. The AgeI/EcoRI fragment containing amino acid residues 350−805 was excised from the Y296H mutant and replaced with the corresponding fragment from each of the other zfAHR1a mutants (386, 388, and 386 and 388). All mutant zfAHR1a constructs were fully sequenced.

Zebrafish AHR and ARNT proteins were expressed in vitro using the T3-coupled (for pBKCMV constructs) or T7-coupled (for pcDNA3.1 constructs) TNT-Quick Coupled Reticulocyte Lysate Systems (Promega) following the manufacturer's recommendations. AHR ligand binding was assessed using unlabeled proteins by velocity sedimentation (sucrose gradient centrifugation) analysis in a vertical tube rotor as described previously.[51] The TNT reaction mixtures were incubated overnight at 4 °C with 8 nM [³H]TCDD; nonspecific binding

was assessed using reaction mixtures containing an empty vector (unprogrammed lysate).[51]

For DNA binding analysis, aliquots (1.5 μL) of the indicated in vitro-expressed wild-type or mutant AHR and ARNT were combined with 7 μL of MEDG [25 mM MOPS-NaOH (pH 7.5), 1 mM EDTA, 1 mM DTT, and 10% glycerol] or MEDGK (MEDG supplemented with 150 mM KCl) buffer and incubated in the presence of 20 nM TCDD [or 1% (v/v) DMSO] for 1.5−2 h at room temperature. For zfAHRs, DNA binding analysis was conducted using zfARNT1c because preliminary analyses revealed that it resulted in a greater amount of TCDD-dependent DNA binding versus that obtained using zfARNT2b (data not shown). The mouse DRE3-containing oligonucleotide was labeled with [³²P]ATP (Perkin-Elmer) and DNA binding (gel retardation) analysis conducted as previously described,[7] except that the amount of KCl in the DNA binding incubation was adjusted to a final concentration of 200 mM. DRE-bound complexes were separated in native polyacrylamide gels, and constitutive and inducible protein−DNA complexes in the dried gel were quantitated using a Fujifilm FLA9000 imager with Multi Gauge software. For protein expression analysis, zebrafish AHR and ARNT constructs were expressed using the TNT system in the presence of [³⁵S]methionine and aliquots subjected to sodium dodecyl sulfate−polyacrylamide gel electrophoresis (PAGE), followed by fluorography. The amount of radioactivity contained in the bands was determined by liquid scintillation counting of the excised bands or by imaging analysis using a Fujifilm FLA9000 with Multi Gauge software.

Transient transfection studies in COS-7 cells were conducted to analyze ligand-dependent transcriptional activation by wild-type and mutant zfAHRs. COS-7 cells were obtained from the American Type Culture Collection (Manassas, VA) and maintained in DMEM (Sigma, St. Louis, MO) supplemented with fetal calf serum (final concentration of 10%) at 37 °C under 5% CO_2. Cells were plated at a density of 5×10^4 cells/well in 48-well plates, and transfections were conducted in triplicate 24 h after cells had been plated. DNA and Lipofectamine 2000 reagent (Invitrogen, Carlsbad, CA) each were diluted in serum-free DMEM, and a total of approximately 300 ng of DNA was complexed with 1 μL of Lipofectamine 2000. The mixture was then added to cells in DMEM with serum. Cells were dosed 5 h after transfection with either DMSO or TCDD (final concentration of 10 nM) at a final DMSO concentration of 0.5%. *Renilla* luciferase (pGL4.74, Promega, Madison, WI) was used as the transfection control. The following amounts of transfected DNA were found: 5 ng each of the AHR expression constructs, 25 ng of ARNT2b, 20 ng of pGudLuc6.1, and 3 ng of pGL4.74. The total amount of transfected DNA was kept constant by addition of the pcDNA3.1 vector with no insert. Cells were lysed 18 h after being dosed, and luminescence was measured using the Dual Luciferase Assay kit (Promega) in a TD 20/20 luminometer (Turner Designs, Sunnyvale, CA). The final luminescence values were expressed as a ratio of the firefly luciferase units to the *Renilla* luciferase units.

■ **RESULTS AND DISCUSSION**

Selection of AHR Sequences. Sixteen AHRs (from 12 different species) with known TCDD binding affinities (K_d) were selected for the generation of the PASB LBD homology models with the goal of comparative analysis of their structural and chemical characteristics and ligand binding cavities. The

names, accession numbers, and relative TCDD binding affinity classification of the various AHRs used in this analysis are listed in Table 1. Among these AHRs, the C57BL/6 mouse mAHR has been commonly used as the reference AHR for purposes of comparison in many studies reporting AHR affinity values from one or several species. The use of a reference AHR in affinity measurements was necessary for these studies because the resulting values usually vary depending on the experimental system, experimental conditions, and ligand binding protocol. Accordingly, TCDD binding affinity estimates for the C57BL/6 mAHR, which is used as the basis for comparisons, are reported to range between 6 pM and 2.4 nM; this is considered to be high affinity.[52−57]

Those AHRs with an affinity for TCDD equal to or greater than that of the C57BL/6 mAHR were classified as having "high" TCDD binding affinity; these included rat, hamster, rabbit, guinea pig, beluga whale, harbor seal, and chicken AHRs (Table 1). Those AHRs with TCDD binding affinity that was consistently 3−10-fold lower than that of the C57BL6 mAHR were designated as having "medium" binding affinity (Table 1) and included DBA mice and human AHRs.[52,54,57,58] The tern AHR also demonstrated a TCDD binding affinity approximately 4−6-fold lower than that of the high-affinity mAHR and chicken AHR, but because binding of [³H]TCDD to this AHR was particularly sensitive to washes with detergent-containing buffer,[53] it was classified as an AHR with "medium/low" affinity (Table 1).

Molecular analysis of several fish species revealed that many contain multiple distinct AHR genes and gene products that vary in their affinity for TCDD.[59] For example, killifish contain at least two distinct AHRs, with kfAHR1a having low affinity for TCDD[60] and kfAHR2a having a medium affinity for TCDD (unpublished results). In contrast, the zebrafish contains three distinct AHRs (zfAHR1a, zfAHR1b, and zfAHR2[28,29,49]). While zfAHR2 has a high affinity for TCDD ($K_d \sim 1$ nM), that for zfAHR1b is lower, although it could not be quantitatively determined because of experimental limitations.[29] However, on the basis of the approximately 8-fold lower potency of TCDD-dependent activation of transcription in COS-7 cells transiently transfected with zfAHR1b, compared to those containing zfAHR2, zfAHR1b is designated to have a medium TCDD binding affinity.[29] Interestingly, in contrast to zfAHR2 and zfAHR1b, zfAHR1a did not demonstrate any detectable [³H]TCDD binding or a transcriptional response to TCDD.[28,29]

Homology Models and Binding Cavities. Structural models of the AHR LBDs of the first seven mammalian AHRs in Table 1 were previously obtained by homology modeling,[17,18] and structure prediction of the nine remaining sequences was performed as previously described.[18] A multiple-sequence alignment of the modeled regions (107 residues corresponding to the region of residues 278−384 of mAHR) is presented in Figure S1 of the Supporting Information. The HIF-2α and ARNT structures were used as templates because these were the available PAS domains with the highest degree of sequence identity with AHR PASB (HIF-2α in the range of 25−30% and ARNT of ~20%, in the aligned regions). For each target sequence, the model with the lowest value of the MODELLER objective function was selected for the subsequent analysis. PROCHECK validation indicated a good stereochemical quality for all the models, with 85−94% of residues belonging to the most favored areas of the Ramachandran plot and the overall G-factors ranging from

−0.15 to −0.05 (this index ranges from −0.5 to 0.3 for structures determined at 1.5 Å resolution). Moreover, the ProSA z-scores were between −3.29 and −5.25, within the range of values for native protein structures of similar size.

A first comparison of the structural characteristics of the whole set of models indicated that the overall fold was well conserved, as shown in the top part of Figure 1 by the
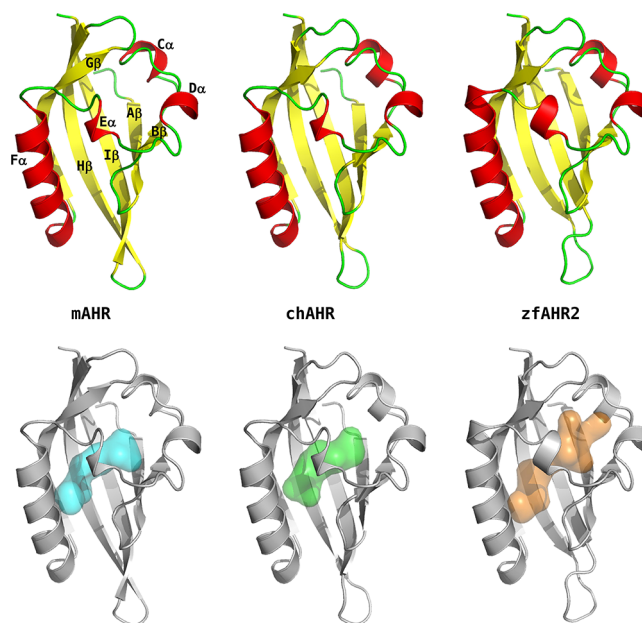

Figure 1. Cartoon representation of the homology models of three AHR LBDs with high affinity for TCDD, representative of each class. In the top row, mouse (mAHR), chicken (chAHR), and zebrafish (zfAHR2) AHR cartoons are colored according to the secondary structure attribution obtained from DSSPcont[45] (red for helices and yellow for β-strands). The secondary structure elements of the mAHR are labeled according to the nomenclature generally adopted for the PAS structures. In the bottom row, cartoons are colored gray, and the molecular surfaces that include the consensus cavity of the high-affinity mammalian AHRs (cyan), the chAHR cavity (green), and the zfAHR2 cavity (orange) are shown. The representations of the cavity surfaces were produced with PyMOL.[47]

representative models of the mAHR, chAHR, and zfAHR2 and, in more detail, in Figure S2 of the Supporting Information by the superimposition of the main chains of the 16 models. A small variability is observed only in the loops encompassing a residue insertion (DE loop) and a two-residue deletion (HI loop) of the global alignment with the templates.[17] The high degree of structural conservation among the AHR models was also confirmed by the low values of the root-mean-square distance (RMSD) between each model and the reference mAHR model (<1 Å on the Cα atoms). Moreover, the secondary structure attribution was highly consistent, with slight differences only in some connecting loops (see the representative models in Figure 1 and secondary structure attribution for all models in Figure S1 of the Supporting Information).

The analysis of structural pockets and cavities, performed by the CASTp server, indicates the presence of a buried cavity in the core of each modeled domain. These cavities have internal volumes ranging from 300 to 600 Å³, which is within the range (100−800 Å³) commonly observed in protein binding pockets or cavities.[61] Given the somewhat inaccurate assignment of
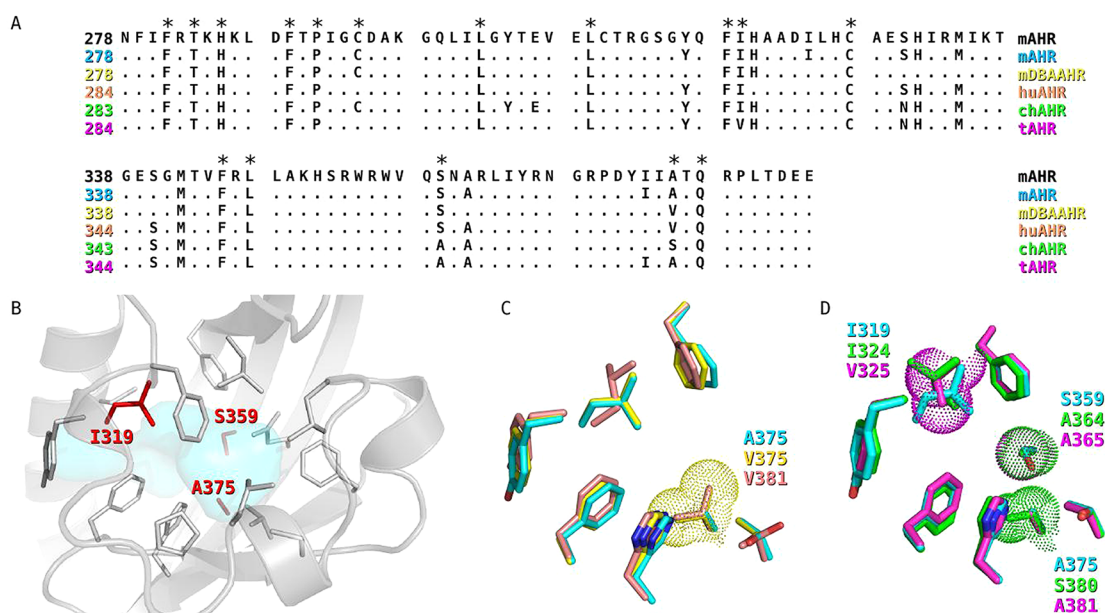
Figure 2. Ligand binding cavities of mammalian and avian AHRs. (A) Sequence alignment of selected mammalian and avian AHRs. Except for the mAHR (taken as a reference), only the residues identified by the CASTp server[48] as internal to the binding cavities are shown. Internal residues conserved in all mammalian AHRs with a high affinity for TCDD are indicated by asterisks. (B) Cartoon representation of the modeled mAHR LBD. The internal residues conserved in all high-affinity mammalian AHRs are shown as gray sticks, and the residues that are not conserved in mammalian and avian AHRs with medium or low affinity for TCDD are labeled and shown as red sticks. The molecular surface of the consensus cavity for mammalian AHRs is colored cyan. (C) Stick representation of the mAHR (cyan), mDBAAHR (yellow), and huAHR (pink) residues in the TCDD-binding fingerprint positions.[18] Steric hindrance of unconserved residues is shown as Van der Waals spheres around the side chains. (D) Stick representation of the residues of the avian AHRs (chAHR colored green and tAHR colored magenta) in the TCDD-binding fingerprint positions, compared to those of the mAHR (cyan). van der Waals spheres are shown around the side chains of unconserved residues.

internal side chain conformations associated with the homology modeling procedure, the volume of a given cavity alone cannot be used reliably to predict ligand accessibility. However, the analysis of internal side chains lining the cavity (obtained from the CASTp analysis) can provide insights into their possible steric and physicochemical interactions with the bound ligand. This analysis helps in our understanding of the role of amino acids at key positions that were previously demonstrated to affect TCDD binding affinity in the mammalian and avian LBDs,[52,53,57] as well as to form hypotheses about their role in the fish LBDs.

One avenue to interspecies analysis of LBD properties is comparison of the cavities of the highest-affinity receptors in each class. For the mammalian AHRs with relatively high affinity for TCDD (first seven AHRs in Table 1), a "consensus cavity" was previously defined as the cavity delimited by the internal residues (obtained by CASTp) that are conserved in all the modeled LBDs.[18] This can be viewed as the internal space shared by all these domains, and as such, it represents the internal space required for optimal binding of TCDD to mammalian AHRs. The cavities of the chAHR and zfAHR2, both with high affinity for TCDD (Table 1), were taken as reference cavities for avian and fish AHRs. The molecular surfaces that include the selected cavities are shown in Figure 1 (bottom row). The consensus cavity for the high-affinity mammalian and the chAHR cavity are very similar in shape and size, and as described below, they also share the same internal conserved residues (see Figure 2A). In contrast, the cavity of the high-affinity fish AHR is characterized by a larger number of internal residues (see Figure 3A), associated with a more elongated shape at both sides (delimited by the Fα helix on one side and the C-terminal β-strands on the other). These distinct

characteristics suggest a slightly different TCDD binding mode for fish AHRs.

Mammalian and Avian AHR LBD Models. In high-affinity mammalian AHRs, seven internal residues have been shown to constitute the "TCDD-binding fingerprint" [i.e., the residues identified by site-directed mutagenesis and functional analysis of the mAHR LBD as being necessary for optimal TCDD binding[18] (Figure 2B,C)]. Of these, Ala375 in the C57BL/6 mAHR has been demonstrated to be essential for optimal TCDD binding, because its mutation to valine[17,62] or natural occurrence as valine in the DBA mouse AHR or in the human AHR (V381)[52,57] results in a decreased affinity for TCDD. The position of this amino acid relative to the other fingerprint residues within the internal cavity is illustrated in Figure 2B. When this amino acid is mutated to Val, it introduces steric hindrance at this end of the modeled cavity (Figure 2C), effectively decreasing the cavity volume and potentially affecting interactions of the ligand with other fingerprint residues.[17,18] Thus, a decrease in the internal cavity volume (below that of the consensus cavity) appears to correlate with the decreased TCDD binding affinity observed with AHRs containing other amino acids at position 375.[17,62]

For avian AHRs, the internal residues of the chAHR and tAHR LBD are shown in Figure 2A. Previously, the difference in TCDD binding affinity between the chAHR (high affinity for TCDD) and tAHR (medium/low affinity for TCDD) was attributed to two amino acid substitutions, I324/V325 and S380/A381.[53] Both these substitutions involve residues that are internal to the modeled cavities and that belong to the TCDD-binding fingerprint for mammalian AHRs.[18] Because neither of these substitutions significantly changes the shape or size of the internal cavity in the modeled LBD structures (Figure 2D), it is
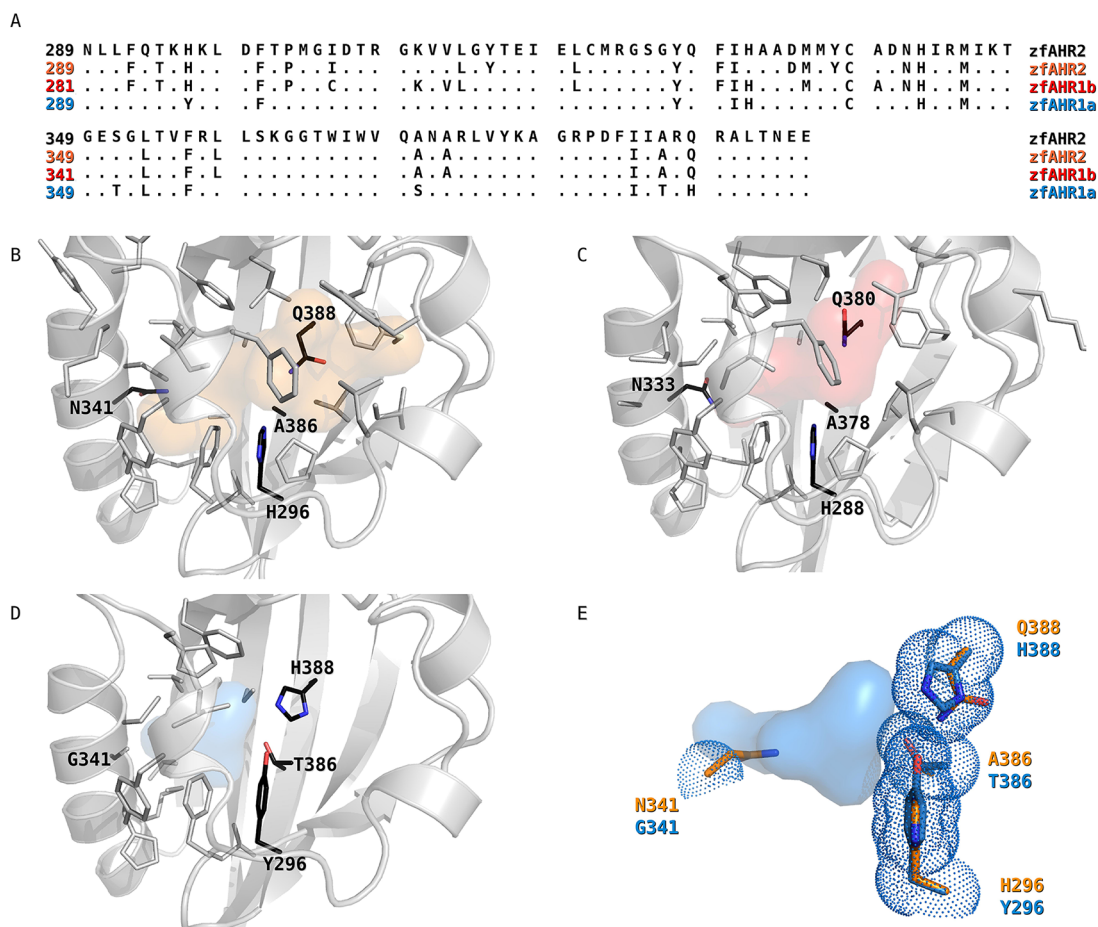
A

```
289 NLLFQTKHKL DFTPMGIDTR GKVVLGYTEI ELCMRGSGYQ FIHAADMMYC ADNHIRMIKT    zfAHR2
289 ...F.T.H.. .F.P..I... ....L.Y... .L......Y. FI...DM.YC ..NH..M...    zfAHR2
281 ...F.T.H.. .F.P..C... .K.VL..... .L......Y. FIH...M..C A.NH..M...    zfAHR1b
289 ......Y... .F........ .......... .......... ...Y. .IH...... C ...H..M...    zfAHR1a

349 GESGLTVFRL LSKGGTWIWV QANARLVYKA GRPDFIIARQ RALTNEE                  zfAHR2
349 ....L..F.L .......... ..A.A..... ....I.A.Q .......                  zfAHR2
341 ....L..F.L .......... ..A.A..... ....I.A.Q .......                  zfAHR1b
349 ..T.L..F.. .......... ..S....... ....I.T.H .......                  zfAHR1a
```


Figure 3. Ligand binding cavities of fish AHRs. (A) Sequence alignment of zfAHR2, zfAHR1b, and zfAHR1a. Except for zfAHR2 (taken as a reference), only the residues identified by the CASTp server[48] as internal to the binding cavities are shown. (B) Cartoon representation of the modeled zfAHR2 LBD. The internal residues are shown as gray sticks, and the residues that are different in zfAHR1a (lacking TCDD binding) are labeled and shown as black sticks. The molecular surface of the internal cavity is colored orange. (C) Cartoon representation of the modeled zfAHR1b LBD. The internal residues are shown as gray sticks, and the residues that are different in zfAHR1a are labeled and shown as black sticks. The molecular surface of the internal cavity is colored red. (D) Cartoon representation of the modeled zfAHR1a LBD. The internal residues are shown as gray sticks, and residues that are different with respect to the zfAHRs that bind TCDD are labeled and shown as black sticks. The molecular surface of the truncated zfAHR1a cavity is colored blue. (E) The steric hindrance of Tyr296, Thr386, and His388 of zfAHR1a (shown as blue van der Waals spheres) results in a truncated internal cavity (blue). The corresponding residues in high-affinity TCDD-binding zfAHR2 are colored orange.

conceivable that TCDD binding in the chAHR LBD may be stabilized by specific interactions with amino acids in or adjacent to these positions. Accordingly, hydrophobic stabilization by the long Ile319 side chain (corresponding to position 324 or 325 in the chAHR or tAHR, respectively) has been previously suggested to be necessary for optimal TCDD binding by mAHR.[18] Therefore, Ile324 in the chicken AHR LBD may stabilize bound TCDD to a greater extent than Val325 present in the tAHR LBD. The role of chicken Ser380 is less clear, because both the high-affinity mAHR and the medium/low-affinity tAHR have Ala at this position.[53] It is possible that optimal electrostatic interactions with the TCDD molecule needed for high-affinity binding require the presence of a polar residue, like Ser, in the region defined by the faced Ser359–Ala375 residue pair in mAHR or Ala364–Ser380 residue pair in chAHR. Binding with the tAHR (Ala365–Ala381) lacks this stabilizing effect (Figure 2D). Further studies will be required to understand the underlying mechanism of the A381S-dependent stabilization of binding of TCDD to the tAHR. Nevertheless, these modeling results demonstrate that residues shown to be critical for binding play evolutionarily conserved roles as part of the ligand-binding cavities of AHRs in mammals and birds.

Fish AHR LBD Models. The analyses described above and previous mutagenesis results[17,18] help to elucidate the importance that the internal cavity size and/or specific amino acid interactions may have in determining TCDD binding affinity. Three zebrafish AHRs have been described (zfAHR1a, zfAHR1b, and zfAHR2), and while zfAHR2 and zfAHR1b can bind TCDD with high and medium affinity, respectively, zfAHR1a fails to bind TCDD.[28,29] As expected, TCDD can stimulate gene expression by zfAHR2 and zfAHR1b, but not by zfAHR1a.[28,29] A previous homology modeling study suggested that the inability of zfAHR1a to bind TCDD was caused by the presence of internal cavity residues different from those in zfAHR2 that decreased the volume and altered the polarity of the binding pocket itself.[20]

Comparison of the internal residues in the zfAHR2 and zfAHR1b modeled cavities (Figure 3A–C) indicates that, while most of these residues occupy corresponding positions and are conserved in the two AHRs, a small group lies in different positions. These variations result in differences in the size and
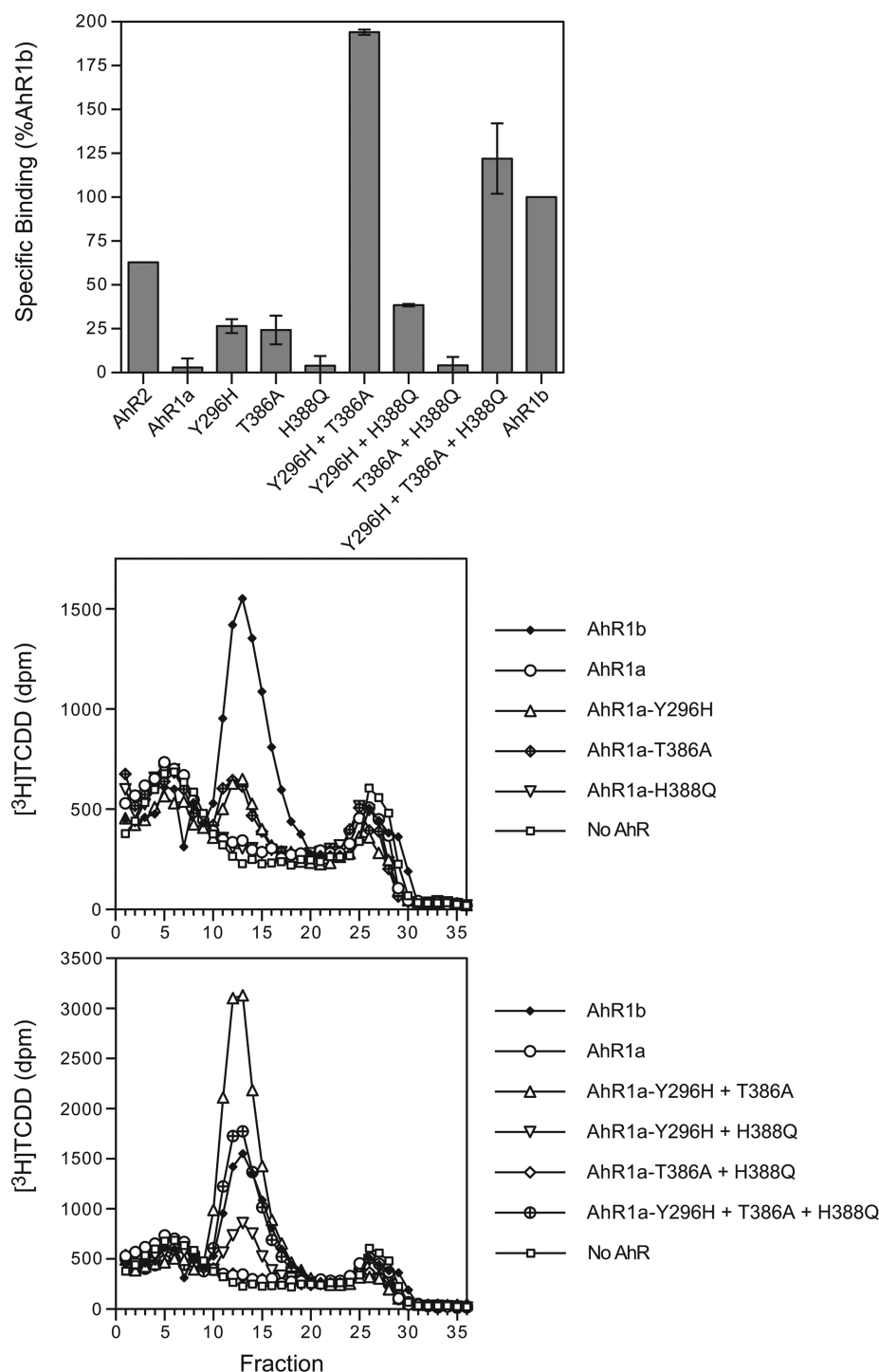
Figure 4. [³H]TCDD-specific binding to wild-type zebrafish AHR1a, AHR1b, and AHR1a containing various mutations. Wild-type and mutant zfAHRs were synthesized in vitro and subjected to [³H]TCDD ligand binding analysis by sucrose density centrifugation as described in Experimental Procedures. Specific binding is expressed as a percentage of the specific binding to AHR1b, measured in the same experiment. The top panel shows results compiled from three experiments, with two or three replicate samples analyzed for each AHR. The bottom panels show representative results from one of the experiments in which all AHRs were analyzed. Note the difference in scale in the two panels.

shape of the two cavities and, in particular, a slightly reduced space available for the ligand in zfAHR1b. This steric characteristic is also observed in the modeled cavities of the other two fish AHRs with low or medium TCDD binding affinity (kfAHR1a or kfAHR2a, respectively), and it may explain the reduced level of binding of these AHRs with respect to that of zfAHR2.

Comparison of the LBD of the high-affinity binding zfAHR2 to that of zfAHR1a, which does not bind TCDD,[28,29] revealed a number of different residues, but only four amino acid differences were identified among the internal residues of these LBDs (Figure 3A,D,E). These amino acid differences (H296Y, N341G, A386T, and Q388H) result in a dramatically shortened internal cavity in the zfAHR1a model (Figure 3D,E), as a consequence of the strong steric hindrance of the side

chains of three of the residues in zfAHR1a (Tyr296, Thr386, and His388) that causes a break in the internal space available to TCDD, limiting its access to the binding cavity. This was also confirmed by the smaller calculated volume (~300 Å^3) and truncated shape of this cavity determined by CASTp in comparison to the internal cavity in zfAHR2 (~600 Å^3), which spans the entire domain fold (Figure 3B). Moreover, the presence of different inter-residue interactions in the central part of the cavity may further limit the access of the ligand as the Tyr296, Thr386, and His388 residues would create a different electrostatic field, and the two facing hydroxyl groups of Tyr296 and Thr386 may generate a network of hydrogen bonds among the side chains.

zfAHR1a LBD Mutagenesis and Functional Analysis. While our analysis and those of Bisson et al.[20] suggest that the steric and electrostatic effects from the side chains of Tyr296, Thr386, and His388 are responsible for the loss of binding of TCDD to zfAHR1a, this has not been confirmed experimentally. Accordingly, to test this hypothesis and more generally to evaluate the ability of homology modeling to predict AHR structure−function relationships, we introduced individual and multiple mutations (Y296H, T386A, and/or H388Q) into zfAHR1a and assessed the ligand (TCDD) binding and ligand-dependent transformation and DNA binding of the mutant AHRs. These specific amino acid substitutions change the specific zfAHR1a residues into those present in zfAHR2 and, on the basis of our homology model, are expected to increase the internal cavity volume and restore the electrostatic environment of the LBD.

Ligand ([^{3}H]TCDD)-specific binding to wild-type and mutant in vitro-synthesized zfAHR1a proteins was conducted using sucrose density centrifugation. The specific mutations did not affect the level of protein synthesized in vitro from these mutant zfAHR constructs (Figure S3 of the Supporting Information). The results of the ligand binding analyses reveal that two of the single mutations, Y296H and T386A, resulted in partial restoration of specific binding of [^{3}H]TCDD to zfAHR1a (Figure 4). Interestingly, [^{3}H]TCDD-specific binding to zfAHR1a containing the Y296H/T386A double mutation was completely restored, and the amount of binding was 2−3 times greater than that observed for fully functional zfAHR1b or zfAHR2. No increase in the level of [^{3}H]TCDD-specific binding was observed with the H388Q mutation, and inclusion of this mutation had a negative effect on ligand binding restoration when combined with a T386A mutation but had no effect on AHRs containing the Y296H mutation (Figure 4). While the underlying mechanism of the increased level of ligand binding of zfAHR1a containing the Y296H/T386A double mutation is unclear, it is possible that the enhanced binding may result from the increased stability of the AHR LBD and/or AHR protein complex. Given our recent results indicating that one of the binding sites of the AHR chaperone protein hsp90 is contained within the AHR LBD,[21] one can envision that an increased level of binding and/or stability of hsp90 within the LBD could further stabilize the AHR, leading to weakened inactivation of AHR ligand binding activity and consequently an increase in the overall amount of [^{3}H]TCDD-specific binding. Whether these mutations result in an increase in AHR ligand binding affinity and/or an increase in functional AHRs that can bind ligand remains to be determined. However, the stabilizing effects of Y296H and T386A mutations on [^{3}H]TCDD-specific binding are consistent with their predicted effect of opening the ligand binding cavity. Overall, the

mutagenesis data confirm the predictions made from comparative analysis of LBD models of the zebrafish AHRs and demonstrate experimentally the importance of amino acids at positions 296 and 386 in facilitating TCDD binding.

The results described above demonstrate that insertion of two mutations (Y296H and T386A) can restore ligand binding to zfAHR1a; however, these analyses do not determine whether these mutations also restore the ability of zfAHR1a to undergo the ligand-dependent events necessary for AHR transformation and binding to DRE-containing DNA. Accordingly, wild-type and mutant zfAHRs were incubated in the absence or presence of 20 nM TCDD, and their ability to transform and bind to DNA was determined by gel retardation analysis (Figure 5A).
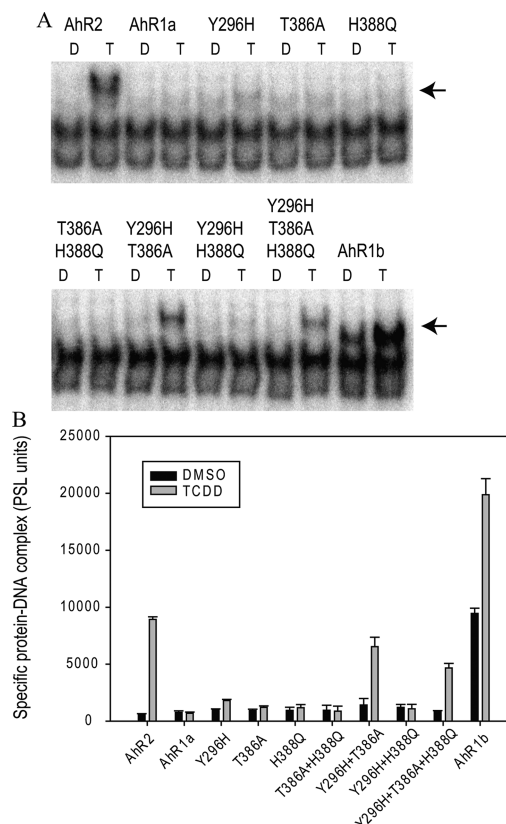

Figure 5. Effect of site-directed mutagenesis of AHR1a on its ability to transform and bind to DNA in a TCDD-inducible manner. (A) Wild-type zfAHR2, zfAHR1b, and zfAHR1a containing various mutations were synthesized in vitro and incubated in the presence of DMSO (D) or 20 nM TCDD (T), and transformation and DNA binding were assessed by gel retardation analysis as described in Experimental Procedures. The arrow indicates the position of the induced protein:DNA complex. (B) Constitutive and inducible protein−DNA complexes in the dried gel were quantitated using a Fujifilm FLA9000 imager with Multi Gauge software, and values represent the mean ± standard deviation of triplicate binding reactions. A typical gel retardation analysis is shown.

Similar to the ligand binding results described above, TCDD-dependent transformation and DNA binding were observed with zfAHR1a containing the Y296H/T386A double mutation as well as that containing the Y296H/T386A/H338Q triple mutation, with the level of DNA binding by the triple mutant zfAHR1a lower than that of the double mutant. A small but significant increase in the level of TCDD-dependent DNA binding was observed with zfAHR1a containing the Y296H

mutation, but not that with the T386A or H388Q mutation. Overall, these results suggest that even though partial restoration of ligand binding occurs (~50%) with zfAHR1a containing the Y296H or T386A mutation, the ligand-dependent change in the AHR necessary to stimulate AHR transformation and ARNT dimerization fails to occur. Further studies of these mutations may provide insights into the mechanisms by which ligand binding triggers AHR activation. Interestingly, while the levels of both constitutive and TCDD-inducible DNA binding by zfAHR1b were dramatically higher than those of zfAHR2 or zfAHR1a containing the double mutation, quantitatively, the amounts of TCDD-dependent enhancement of DNA binding by zfAHR2 and zfAHR1b were similar (Figure 5B). The reason for the increased level of constitutive DNA binding by the zfAHR1b:zfARNT1c complex is not clear. Interestingly, these DNA binding analyses also revealed for the first time that zfAHR1b:ARNT:DRE complexes can migrate significantly faster in native PAGE gels than complexes formed with AHR2 or the functional AHR1a mutants (Figure 5A). The reasons for these differences in migration remain to be determined. However, it is very likely that the significant differences in the overall size and charge of each of the zfAHRs (AHR2 consists of 1027 amino acids with a calculated pI of 7.3, zfAHR1b 940 amino acids with a calculated pI of 6.35, and mut_zfAHR1a 787 amino acids with a calculated pI of 8.05), their relatively low degree of amino acid identity (~40%),[28,29] differences in the overall protein conformation and/or structure of each zfAHR, and ultimately their respective zfAHR1b:ARNT:DRE complexes would be contributing factors. Overall, the site-directed mutagenesis results reveal that the mutations that can fully restore ligand (TCDD) binding activity can also restore TCDD-dependent transformation and DNA binding. These results also demonstrate that the dimerization and DNA binding interfaces of zfAHR1a appear to be functional, and the apparent lack of TCDD-dependent zfAHR1a activation likely results, at least in part, from impaired TCDD binding as a result of selected substitutions within its LBD.

The inability of zfAHR1a to bind TCDD or mediate TCDD-dependent gene expression or toxicity in vivo led to the suggestion that it may be an AHR pseudogene instead of a functional AHR gene.[29] Not only does zfAHR1a have an altered LBD that fails to bind TCDD, but previous domain swapping experiments between zfAHR1a and zfAHR2 suggested that the zfAHR1a transactivation domain was also nonfunctional as it failed to confer TCDD-dependent gene expression in transfection experiments when fused to the N-terminal end of zfAHR2 containing functional ligand binding, DNA binding, and dimerization domains.[28] However, the functional activity of this transactivation domain may be zfAHR1a-specific and may require it to have a functional LBD. Accordingly, to test this, we examined the TCDD-dependent transcriptional activity of wild-type and mutant zfAHR1a in COS-7 cells transiently cotransfected with AHR-responsive luciferase reporter plasmid pGudLuc6.1. While TCDD induced luciferase activity in cells transfected with wild-type zfAHR1b or zfAHR2, no TCDD induction was observed in cells cotransfected with wild-type or mutant zfAHR1a, irrespective of its ability to bind TCDD or exhibit TCDD-dependent DNA binding (Figure 6). Together, these results extend previous studies demonstrating that the zfAHR1a transactivation domain is nonfunctional by demonstrating that even changes that dramatically restore ligand binding and DNA binding in a
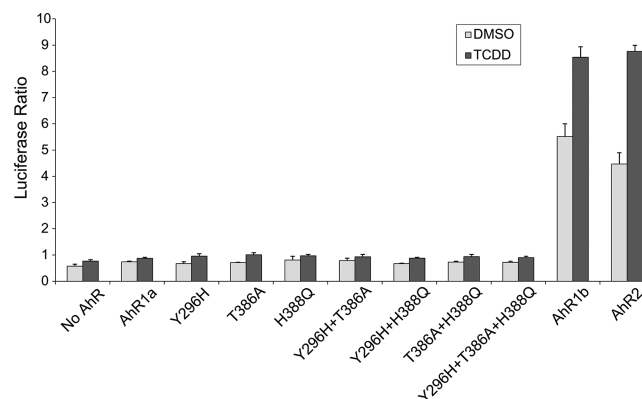

Figure 6. Effect of site-directed mutagenesis of AHR1a on its ability to activate transcription. COS-7 cells were transfected with expression constructs for zebrafish ARNT2b (25 ng), pGudLuc6.1 (20 ng), pGL4.74 (transfection control), and the indicated AHR expression constructs (5 ng). "No AHR" indicates transfection with only the reporter construct and the transfection control. The cells were exposed to dimethyl sulfoxide or TCDD (10 nM). The luciferase activity was measured in a luminometer, and the relative luciferase units were calculated by normalizing the firefly luciferase activity to the transfection control *Renilla* luciferase.

native context (i.e., not a chimeric protein) are insufficient to restore the ligand-dependent transactivation function of this AHR.

Given the dramatic structural diversity of AHR ligands, combined with recent evidence of differential binding of such structurally diverse ligands with different residues within the AHR ligand binding cavity,[3,11−14] it is possible that while zfAHR1a is unable to bind TCDD-like chemicals, it may still bind and be activated by chemicals that are structurally distinct from TCDD. In fact, molecular docking studies using the AHR LBD homology model identified leflunomide as a possible unique ligand for zfAHR1a.[63] In addition, analysis in transgenic zebrafish in which the various zfAHRs had been knocked out or knocked down revealed that leflunomide could induce CYP1A expression in a zfAHR1a-dependent manner.[63] These studies suggested that although leflunomide was predicted to bind differently within the LBDs of zfAHR1a and zfAHR2, it was still able to stimulate the same gene induction response and thus must contact common key residues critical for activation of AHR transformation events. Other studies also suggest that zfAHR1a may be functional with certain ligands; Incardona and co-workers have reported that knockdown of zfAHR1a provides protection against the embryotoxicity of pyrene.[64] These results indicate not only that the transactivation domain of zfAHR1a is functional but also that its activation appears to occur by a ligand-selective mechanism that is distinct from that of the zfAHR2 transactivation domain. How zfAHR1a is activated by leflunomide and whether other AHR ligands can also bind and activate this AHR remain to be elucidated.

Overall, our findings demonstrate that direct comparison of homology models of AHR LBDs from different species is able to reveal the evolutionary conservation of some key features in the binding cavities of AHRs with high TCDD binding affinity. Moreover, our experimental results verify the ability of the modeling approach to predict the specific residues that play a critical role in TCDD binding. More generally, the results of this study indicate that comparative analysis of homology models can provide important structural insights into ligand-specific mechanisms of AHR binding and activation that may

help to explain some of the dramatic ligand- and species-specific differences in AHR function. Such a mechanistic understanding will inform efforts to explore the AHR as a target for therapeutic intervention and to use the AHR as a molecular biomarker of susceptibility in risk assessment.

■ ASSOCIATED CONTENT

Ⓢ Supporting Information

Oligonucleotide sequences used for site-directed mutation of zebrafish AHR1a by polymerase chain reaction (Table S1), sequence alignment and secondary structure attribution of 16 AHRs (Figure S1), ribbon overlay representation of the PASB LBD structure of the 16 AHRs selected for the comparative analysis (Figure S2), and in vitro expression levels of wild-type and mutant zfAHRs, zfARNTs, and mAHR and mARNT (Figure S3). This material is available free of charge via the Internet at http://pubs.acs.org.

■ AUTHOR INFORMATION

Corresponding Author
*Telephone: (530) 752-3879. Fax: (530) 752-3394. E-mail: msdenison@ucdavis.edu.

Notes
The authors declare no competing financial interest.

■ ACKNOWLEDGMENTS

■ ABBREVIATIONS

AHR, aryl hydrocarbon receptor; mAHR, *M. musculus* (mouse) aryl hydrocarbon receptor; zfAHR, *D. rerio* (zebrafish) aryl hydrocarbon receptor (all other AHR species abbreviations are listed in Table 1); ; ARNT, aryl hydrocarbon receptor nuclear translocator; bHLH, basic helix−loop−helix; DMSO, dimethyl sulfoxide; DMEM, Dulbecco's minimal essential medium; DRE, dioxin responsive element; HAHs, halogenated aromatic hydrocarbons; HIF-2a, hypoxia-inducible factor 2α; LBD, ligand binding domain; MEDG, 25 mM MOPS-NaOH (pH 7.5), 1 mM EDTA, 1 mM DTT, and 10% glycerol; NMR, nuclear magnetic resonance; PAS, Per-ARNT-Sim; PDB, Protein Data Bank; RMSD, root-mean-square distance; TCDD, 2,3,7,8-tetrachlorodibenzo-*p*-dioxin.

■ REFERENCES

(1) Beischlag, T. V., Morales, J. L., Hollingshead, B. D., and Perdew, G. H. (2008) The aryl hydrocarbon receptor complex in the control of gene expression. *Crit. Rev. Eukaryotic Gene Expression 18*, 207−250.

(2) Furness, S. G., and Whelan, F. (2009) The pleiotropy of dioxin toxicity−xenobiotic misappropriation of the aryl hydrocarbon receptor's alternative physiological roles. *Pharmacol. Ther. 124*, 336−353.

(3) Denison, M. S., Soshilov, A. A., He, G., DeGroot, D. E., and Zhao, B. (2011) Exactly the same but different: Promiscuity and diversity in the molecular mechanisms of action of the aryl hydrocarbon (dioxin) receptor. *Toxicol. Sci. 124*, 1−22.

(4) Soshilov, A., and Denison, M. S. (2008) Role of the Per/Arnt/Sim domains in ligand-dependent transformation of the aryl hydrocarbon receptor. *J. Biol. Chem. 283*, 32995−32305.

(5) Hankinson, O. (1995) The aryl hydrocarbon receptor complex. *Annu. Rev. Pharmacol. Toxicol. 35*, 307−340.

(6) Denison, M. S., Seidel, S. D., Rogers, W. J., Ziccardi, M., Winter, G. M., and Heath-Pagliuso, S. (1998) Natural and synthetic ligands for the Ah receptor. In *Molecular Biology Approaches to Toxicology* (Puga, A., and Wallace, K. B., Eds.) pp 393−410, Taylor & Francis, Philadelphia.

(7) Safe, S. (1990) Polychlorinated biphenyls (PCBs), dibenzo-p-dioxins (PCDDs), dibenzofurans (PCDFs), and related compounds: Environmental and mechanistic considerations which support the development of toxic equivalency factors (TEFs). *Crit. Rev. Toxicol. 21*, 51−88.

(8) Denison, M. S., and Nagy, S. R. (2003) Activation of the aryl hydrocarbon receptor by structurally diverse exogenous and endogenous chemicals. *Annu. Rev. Pharmacol. Toxicol. 43*, 309−334.

(9) Nguyen, L. P., and Bradfield, C. A. (2008) The search for endogenous activators of the aryl hydrocarbon receptor. *Chem. Res. Toxicol. 21*, 102−106.

(10) Poland, A., and Knutson, J. C. (1982) 2,3,7,8-Tetrachlorodibenzo-p-dioxin and related halogenated aromatic hydrocarbons: Examination of the mechanism of toxicity. *Annu. Rev. Pharmacol. Toxicol. 22*, 517−542.

(11) Whelan, F., Hao, N., Furness, S. G. B., Whitelaw, M. L., and Chapman-Smith, A. (2010) Amino acid substitutions in the aryl hydrocarbon receptor (AhR) ligand binding domain reveal YH439 as an atypical AhR activator. *Mol. Pharmacol. 77*, 1037−1046.

(12) Xing, Y., Nukaya, M., Satyshur, K., Jiang, L., Stanevich, V., Korkmaz, E. N., Burdette, L., Kennedy, G., Cui, Q., and Bradfield, C. A. (2012) Identification of the Ah-receptor structural determinants for ligand preferences. *Toxicol. Sci. 129*, 86−97.

(13) Zhao, B., Degroot, D., Hayashi, A., He, G., and Denison, M. S. (2010) CH223191 is a ligand-selective antagonist of the Ah (dioxin) receptor. *Toxicol. Sci. 117*, 393−403.

(14) DeGroot, D., He, G., Fraccalvieri, D., Bonati, L., Pandini, A., and Denison, M. S. (2011) AhR Ligands: Promiscuity in Binding and Diversity in Response. In *The Ah Receptor in Biology and Toxicology* (Pohjanvirta, R., Ed.) pp 63−79, John Wiley & Sons, Inc., Hoboken, NJ.

(15) LeCluyse, E. L. (2001) Pregnane X receptor: Molecular basis for species differences in CYP3A induction by xenobiotics. *Chem.-Biol. Interact. 134*, 283−289.

(16) Ngan, C. H., Beglov, D., Rudnitskaya, A. N., Kozakov, D., Waxman, D. J., and Vajda, S. (2009) The structural basis of pregnane X receptor binding promiscuity. *Biochemistry 48*, 11572−11578.

(17) Pandini, A., Denison, M. S., Song, Y., Soshilov, A. A., and Bonati, L. (2007) Structural and functional characterization of the AhR ligand binding domain by homology modeling and mutational analysis. *Biochemistry 46*, 696−708.

(18) Pandini, A., Soshilov, A. A., Song, Y., Zhao, J., Bonati, L., and Denison, M. S. (2009) Detection of the TCDD binding fingerprint within the Ah receptor ligand binding domain by structurally driven mutagenesis and functional analysis. *Biochemistry 48*, 5972−5983.

(19) Motto, I., Bordogna, A., Soshilov, A. A., Denison, M. S., and Bonati, L. (2011) A new aryl hydrocarbon receptor homology model targeted to improve docking reliability. *J. Chem. Inf. Model. 51*, 2868−2881.

(20) Bisson, W. H., Koch, D. C., O'Donnell, E. F., Khalil, S. M., Kerkvliet, N. I., Tanguay, R. L., Abagyan, R., and Kollui, S. K. (2009) Modeling of the aryl hydrocarbon receptor (AhR) ligand binding domain and its utility in virtual ligand screening to predict new AhR ligands. *J. Med. Chem. 52*, 5635−5641.

(21) Soshilov, A., and Denison, M. S. (2011) Ligand displaces heat shock protein 90 from overlapping binding sites within the aryl hydrocarbon receptor ligand-binding domain. *J. Biol. Chem. 286*, 35275–35282.

(22) O'Donnell, E. F., Saili, K. S., Koch, D. C., Kopparapu, P. R., Farrer, D., Bisson, W. H., Mathew, L. K., Sengupta, S., Kerkvliet, N. I., Tanguay, R. L., and Kolluri, S. K. (2010) The anti-inflammatory drug leflunomide is an agonist of the aryl hydrocarbon receptor. *PLoS One 5*, e13128.

(23) Wu, B., Zhang, Y., Kong, J., Zhang, X., and Cheng, S. (2009) In silico predication of nuclear hormone receptors for organic pollutants by homology modeling and molecular docking. *Toxicol. Lett. 191*, 69–73.

(24) Jogalekar, A. S., Reiling, S., and Vaz, R. J. (2010) Identification of optimum computational protocols for modeling the aryl hydrocarbon receptor (AHR) and its interaction with ligands. *Bioorg. Med. Chem. Lett. 20*, 6616–6619.

(25) Murray, I. A., Flaveny, C. A., Chiaro, C. R., Sharma, A. K., Tanos, R. S., Schroeder, J. C., Amin, S. G., Bisson, W. H., Kolluri, S. K., and Perdew, G. H. (2011) Suppression of cytokine-mediated complement factor gen expression through selective activation of the Ah receptor with 3′,4′-dimethoxy-α-naphthoflavone. *Mol. Pharmacol. 79*, 508–519.

(26) Flaveny, C. A., Murray, I. A., Chiaro, C. R., and Perdew, G. H. (2009) Ligand selectivity and gene regulation by the human aryl hydrocarbon receptor in transgenic mice. *Mol. Pharmacol. 75*, 1412–1420.

(27) Aarts, J. M., Denison, M. S., Cox, M. A., Schalk, M. A., Garrison, P. M., Tullis, K., deHaan, L. H., and Brouwer, A. (1995) Species-specific antagonism of Ah receptor action by 2,2′,5,5′-tetrachloro- and 2,2′,3,3′,4,4′-hexachlorobiphenyl. *Eur. J. Pharmacol. 293*, 463–474.

(28) Andreasen, E. A., Hahn, M. E., Heideman, W., Peterson, R. E., and Tanguay, R. L. (2002) The zebrafish (*Danio rerio*) aryl hydrocarbon receptor type 1 is a novel vertebrate receptor. *Mol. Pharmacol. 62*, 234–249.

(29) Karchner, S. I., Franks, D. G., and Hahn, M. E. (2005) AHR1B, a new functional aryl hydrocarbon receptor in zebrafish: Tandem arrangement of ahr1b and ahr2 genes. *Biochem. J. 392*, 153–161.

(30) Altschul, S. F., Madden, T. L., Schaffer, A. A., Zhang, J., Zhang, Z., Miller, W., and Lipman, D. J. (1997) Gapped BLAST and PSI-BLAST: A new generation of protein database search programs. *Nucleic Acids Res. 25*, 3389–3402.

(31) Berman, H. M., Westbrook, J., Feng, Z., Gilliland, G., Bhat, T. N., Weissig, H., Shindyalov, I. N., and Bourne, P. E. (2000) The Protein Data Bank. *Nucleic Acids Res. 28*, 235–242.

(32) Erbel, P. J., Card, P. B., Karakuzu, O., Bruick, R. K., and Gardner, K. H. (2003) Structural basis for PAS domain hetero-dimerization in the basic helix–loop–helix-PAS transcription factor hypoxia-inducible factor. *Proc. Natl. Acad. Sci. U.S.A. 100*, 15504–15509.

(33) Card, P. B., Erbel, P. J., and Gardner, K. H. (2005) Structural basis of ARNT PAS-B dimerization: Use of a common β-sheet interface for hetero- and homodimerization. *J. Mol. Biol. 353*, 664–677.

(34) Kelley, L. A., Gardner, S. P., and Sutcliffe, M. J. (1996) An automated approach for clustering an ensemble of NMR-derived protein structures into conformationally related subfamilies. *Protein Eng. 9*, 1063–1065.

(35) Holm, L., and Park, J. (2000) DaliLite workbench for protein structure comparison. *Bioinformatics 16*, 566–567.

(36) Holm, L., and Sander, C. (1993) Protein structure comparison by alignment of distance matrices. *J. Mol. Biol. 233*, 123–138.

(37) Thompson, J. D., Higgins, D. G., and Gibson, T. J. (1994) CLUSTAL W: Improving the sensitivity of progressive multiple sequence alignment through sequence weighting, position-specific gap penalties and weight matrix choice. *Nucleic Acids Res. 22*, 4673–4680.

(38) Larkin, M. A., Blackshields, G., Brown, N. P., Chenna, R., McGettigan, P. A., McWilliam, H., Valentin, F., Wallace, I. M., Wilm, A., Lopez, R., Thompson, J. D., Gibson, T. J., and Higgins, D. G. (2007) Clustal W and Clustal X version 2.0. *Bioinformatics 23*, 2947–2948.

(39) Sali, A., and Blundell, T. L. (1993) Comparative protein modelling by satisfaction of spatial restraints. *J. Mol. Biol. 234*, 779–815.

(40) Marti-Renom, M. A., Stuart, A. C., Fiser, A., Sanchez, R., Melo, F., and Sali, A. (2000) Comparative protein structure modeling of genes and genomes. *Annu. Rev. Biophys. Biomol. Struct. 29*, 291–325.

(41) Fiser, A., Do, R. K., and Sali, A. (2000) Modelling of loops in protein structures. *Protein Sci. 9*, 1753–1773.

(42) Laskowski, R. A., MacArthur, M. W., Moss, D. S., and Thornton, J. M. (1993) PROCHECK: A program to check the stereochemical quality of protein structures. *J. Appl. Crystallogr. 26*, 283–291.

(43) Sippl, M. J. (1993) Recognition of errors in three-dimensional structures of proteins. *Proteins 17*, 355–362.

(44) Wiederstein, M., and Sippl, M. J. (2007) ProSA-web: Interactive web service for the recognition of errors in three-dimensional structures of proteins. *Nucleic Acids Res. 35*, W407–W410.

(45) Andersen, C. A., Palmer, A. G., Brunak, S., and Rost, B. (2002) Continuum secondary structure captures protein flexibility. *Structure 10*, 175–184.

(46) Kabsch, W., and Sander, C. (1983) Dictionary of protein secondary structure: Pattern recognition of hydrogen-bonded and geometrical features. *Biopolymers 22*, 2577–2637.

(47) *The PyMOL Molecular Graphics System*, version 1.3 (2010) Schrödinger, LLC, New York.

(48) Dundas, J., Ouyang, Z., Tseng, J., Binkowski, A., Turpaz, Y., and Liang, J. (2006) CASTp: Computed atlas of surface topography of proteins with structural and topographical mapping of functionally annotated residues. *Nucleic Acids Res. 34*, W116–W118.

(49) Tanguay, R. L., Abnet, C. C., Heideman, W., and Peterson, R. E. (1999) Cloning and characterization of the zebrafish (*Danio rerio*) aryl hydrocarbon receptor. *Biochim. Biophys. Acta 1444*, 35–48.

(50) Prasch, A. L., Tanguay, R. L., Mehta, V., Heideman, W., and Peterson, R. E. (2006) Identification of zebrafish ARNT1 homologs: 2,3,7,8-tetrachlorodibenzo-p-dioxin toxicity in the developing zebrafish requires ARNT1. *Mol. Pharmacol. 69*, 776–787.

(51) Karchner, S. I., Powell, W. H., and Hahn, M. E. (1999) Identification and functional characterization of two highly divergent aryl hydrocarbon receptors (AHR1 and AHR2) in the teleost *Fundulus heteroclitus*. Evidence for a novel subfamily of ligand-binding basic helix loop helix-Per-ARNT-Sim (bHLH-PAS) factors. *J. Biol. Chem. 274*, 33814–33824.

(52) Ema, M., Ohe, N., Suzuki, M., Mimura, J., Sogawa, K., Ikawa, S., and Fujii-Kuriyama, Y. (1994) Dioxin binding activities of poly-morphic forms of mouse and human aryl hydrocarbon receptors. *J. Biol. Chem. 269*, 27337–27343.

(53) Karchner, S. I., Franks, D. G., Kennedy, S. W., and Hahn, M. E. (2006) The molecular basis for differential dioxin sensitivity in birds: Role of the aryl hydrocarbon receptor. *Proc. Natl. Acad. Sci. U.S.A. 103*, 6252–6257.

(54) Jensen, B. A., and Hahn, M. E. (2001) cDNA cloning and characterization of a high affinity aryl hydrocarbon receptor in a cetacean, the beluga, *Delphinapterus leucas*. *Toxicol. Sci. 64*, 41–56.

(55) Denison, M. S., Wilkinson, C. F., and Okey, A. B. (1986) Ah receptor for 2,3,7,8-tetrachlorodibenzo-p-dioxin: Comparative studies in mammalian and nonmammalian species. *Chemosphere 15*, 1665–1672.

(56) Kim, E. Y., and Hahn, M. E. (2002) cDNA cloning and characterization of an aryl hydrocarbon receptor from the harbor seal (*Phoca vitulina*): A biomarker of dioxin susceptibility? *Aquat. Toxicol. 58*, 57–73.

(57) Poland, A., Palen, D., and Glover, E. (1994) Analysis of the four alleles of the murine aryl hydrocarbon receptor. *Mol. Pharmacol. 46*, 915–921.

(58) Denison, M. S., Hamilton, J. W., and Wilkinson, C. F. (1985) Comparative studies of aryl hydrocarbon hydroxylase and the Ah receptor in nonmammalian species. *Comp. Biochem. Physiol., Part C: Pharmacol., Toxicol. Endocrinol. 80*, 319–324.

(59) Hahn, M. E., Karchner, S. I., Evans, B. R., Franks, D. G., Merson, R. R., and Lapseritis, J. M. (2006) Unexpected diversity of aryl hydrocarbon receptors in non-mammalian vertebrates: Insights from comparative genomics. *J. Exp. Zool., Part A 305*, 693−706.

(60) Hahn, M. E., Karchner, S. I., Franks, D. G., and Merson, R. R. (2004) Aryl hydrocarbon receptor polymorphisms and dioxin resistance in Atlantic killifish (*Fundulus heteroclitus*). *Pharmacogenetics 14*, 131−143.

(61) Liang, J., Edelsbrunner, H., and Woodward, C. (1998) Anatomy of protein pockets and cavities: Measurement of binding site geometry and implications for ligand design. *Protein Sci. 7*, 1884−1897.

(62) Murray, I. A., Reen, R. K., Leathery, N., Ramadoss, P., Bonati, L., Gonzalez, F. J., Peters, J. M., and Perdew, G. H. (2005) Evidence that ligand binding is a key determinant of Ah receptor-mediated transcriptional activity. *Arch. Biochem. Biophys. 442*, 59−71.

(63) Goodale, B. C., La Du, J. K., Bisson, W. H., Janszen, D. B., Waters, K. M., and Tanguay, P. L. (2012) AHR2 mutant reveals functional diversity of aryl hydrocarbon receptors in zebrafish. *PLoS One 7*, e29346.

(64) Incardona, J. P., Day, H. L., Collier, T. K., and Scholz, N. L. (2006) Developmental toxicity of 4-ring polycyclic aromatic hydrocarbons in zebrafish is differentially dependent on AH receptor isoforms and hepatic cytochrome P4501A metabolism. *Toxicol. Appl. Pharmacol. 217*, 308−321.

(65) Karchner, S. I., Franks, D. G., Pandini, A., Soshilov, A. A., Bonati, L., Denison, M. S., and Hahn, M. E. (2011) Testing structure-binding predictions from comparative modeling of the AHR ligand-binding domain: Studies with zebrafish AHR1a. *Toxicol. Sci. 110* (The Toxicologist Supplement), 79 (Abstract 368).